On the Trade-off Between Network Lifetime and k-Connectivity Based Reliability in UWSNs

Muhammed Cobanlar, Huseyin Ugur Yildiz, *Senior Member, IEEE*, Vahid Khalilpour Akram, *Member, IEEE*, Orhan Dagdeviren, *Member, IEEE*, and Bulent Tavli, *Senior Member, IEEE*

***Abstract*—Underwater wireless sensor networks (UWSNs) are utilized for a wide range of monitoring and surveillance applications. Lifetime maximization and maintenance of network reliability are among the most important considerations in the deployment of UWSNs. k-connectivity is a robust approach for reinforcing reliability. However, maintaining k disjoint paths from each sensor node to the BS, inevitably, results in extra energy dissipation, which reduces the network lifetime (NLT). Yet, there is no systematic exploration to determine the extent of lifetime reduction due to the increase in the k value, in the literature, to the best of our knowledge. In this study, we create an optimization framework to be able to explore the trade-off between NLT and k-connectivity based reliability in UWSNs. Through the optimal solutions of the proposed optimization model for a large set of salient parameters, we characterize the inter-play between lifetime and k-connectivity. Our analysis reveals that the k value to be maintained in a UWSN can affect the NLT significantly.**

***Index Terms*—underwater wireless sensor networks, k-connectivity, network lifetime, mixed-integer linear programming, reliability.**

I. Introduction

APPROXIMATELY 70% of the earth's surface is water-covered. Monitoring bodies of water is, therefore, a practical necessity for many applications such as coastal exploration, military tactical underwater surveillance, aquaculture, and long-term pollution monitoring, among others [1]. As the technological developments in communications technology (especially underwater acoustic communications) have reached a certain maturity level; the viability, and efficiency of underwater wireless sensor networks (UWSNs) have become a reality for scientific, industrial, and military applications for more than two decades [2]. A UWSN consists of a plurality of floating submerged sensor nodes, which are deployed over a geographical area to monitor physical phenomena such as temperature, pressure, and humidity. Furthermore, there is, at least, one base station (BS) in a UWSN, which, itself, can also be floating at a certain depth below the water surface or can float on the water surface. Sensor nodes convey the data they acquire to the BS. Early UWSNs, typically, utilize a single-hop communication paradigm, where the sensor nodes transmit the data they acquire from the environment to the BS directly. As the enabling technologies improved, multi-hop communications in UWSNs have become the dominant mode of operation due to the advantages such as extended network area, energy efficiency, and reliability [3].

Energy efficiency and reliability are among the most important performance metrics in UWSNs. Since sensor nodes have limited battery energies and it is difficult or in some cases impossible to replenish the batteries, it is of paramount importance for UWSNs to avoid energy wastage [4]. Reliability, on the other hand, is as important as energy efficiency in UWSNs because underwater as a deployment environment is a harsh medium, and nodes, as well as links, are prone to failure. There are, at least, k disjoint paths from each sensor node to the BS in a k-connected network. Therefore, even if up to $k-1$ paths of a particular sensor node are left nonoperational in such a network, the sensor node, still, is guaranteed to remain connected. As such k-connectivity provides a high degree of network reliability, especially, if the k value is high.

Maintaining a k-connected UWSN requires extra energy to be dissipated to maintain, at least, k disjoint paths originating at each sensor node. As such, there is a trade-off between the level of reliability in terms of k value and network lifetime (NLT) in a k-connected UWSN. k-connectivity in UWSNs is a topic that is scarcely investigated. Indeed, there has been only one study on this topic [5]. Furthermore, the impact of k value on wireless sensor network (WSN) lifetime has also been left uninvestigated in the literature. In fact, the only study that explores the relation between k-connectivity and NLT (in terrestrial sensor networks) is [6], which did not directly investigate the impact of the energy cost of maintaining k-connectivity on NLT. Further elaborations on [6] are presented in Section II.

In this study, we systematically investigate the impact of maintaining a k-connected UWSN on energy dissipation and NLT, which has never been explored in the literature, to the best of our knowledge. We create an optimization framework to model the effects of the k value on UWSN lifetime, which is utilized to characterize the trade-off between k-connectivity and NLT.

The rest of the paper is organized as follows. A concise literature review on k-connectivity and NLT is given in Section II, where the novel contributions of this study in reference to the existing literature are stated. The system model, which encompasses the network representation, energy model, and optimization framework, is presented in Section III. Our analysis based on the results obtained by the solutions of the

M. Cobanlar and B. Tavli are with the Department of Electrical and Electronics Engineering, TOBB University of Economics and Technology, 06520, Ankara, Turkey. (e-mail: {mcobanlar,btavli}@etu.edu.tr).

H. U. Yildiz is with the Department of Electrical and Electronics Engineering, TED University, 06420, Ankara, Turkey (e-mail: hugur.yildiz@tedu.edu.tr)

V. K. Akram and O. Dagdeviren are with the International Computer Institute, Ege University, 35040, Izmir, Turkey. (e-mail: {vahid.akram,orhan.dagdeviren}@ege.edu.tr).

optimization model is provided in Section IV. The conclusions of this study are drawn in Section V.

II. Related Work

Preserving connectivity is one of the main challenges in WSNs, which has been extensively studied from different perspectives. In [7], a probabilistic k-coverage algorithm to maximize NLT by covering a set of points of interest arranged as a regular grid by randomly deployed WSN nodes is proposed. k-coverage is defined as each point of interest being sensed by at least k active nodes (i.e., nodes that are not in sleep mode). Furthermore, active sensor nodes are designed to be connected. However, in this study, the objective is to establish 1-connectivity, as opposed to general k-connectivity (i.e., for $k > 1$).

In general, research on the connectivity robustness of WSNs can be categorized into node deployment, connectivity restoration, and connectivity detection classes. Research on node deployment, typically, is concerned with designing methods or patterns to establish connectivity between the nodes [8], [9], maximize the covered area [10], [11] or extend NLT [12]. Deployment of nodes to the predefined locations [9], [13] and determining the transmission powers of nodes [14], [15] are salient deployment methods to accomplish k-connectivity. Although the deployment of nodes to predefined locations can, potentially, create an efficient k-connected network, it is not always possible to place nodes to specific locations in some applications, especially, in uneven and harsh environments [16]. Increasing transmission powers of sensor nodes can lead to the creation of additional links, which in turn, facilitates the establishment of a k-connected network with the desired k value, however, higher transmission power dissipation can result in more energy consumption and reduce NLT [6].

The first step in any algorithm concerned with k-connectivity is to determine or estimate the k value of the network under consideration [17], [18]. Finding the k value of a given network is a well-known graph theory problem addressed by a plurality of sequential [19] and distributed algorithms [20]–[22]. Detection of the k value of a given network can, potentially, reveals valuable information on the fault tolerance and reliability of the network. An analysis of k-connectivity based reliability of underwater optical wireless networks is presented in [5] considering effects of data rate, wavelength, error probability, transmission power, and node density among others. Most of the studies on the restoration problem propose efficient solutions for the restoration of the lost or weakened connectivity after failure in some nodes or links [23], [24]. After a failure, which decreases the k value of a given network, the k value of the network can be restored to the desired value by placing new sensor nodes to appropriate positions or moving existing nodes to suitable new locations.

NLT, arguably, is the most important performance metric in WSNs. On the other hand, the reliable operation of WSNs is also an important objective, especially for underwater networks [3]. Maintaining k-connectivity is a robust method of achieving network connection reliability, especially for high k values. However, most of the existing studies on k-connectivity deployment, detection, and restoration problems focus on 1-connectivity (i.e., $k = 1$).

In [6], the relationship between the k value and NLT for two specific cases is investigated. In the first case, each sensor node utilizes the optimal transmission power for each of its outgoing links (if the flow on the particular link is non-zero) to transmit data as well as the amount of data to be conveyed on the link. Such an assignment results in the maximum NLT achievable. In the second case, each sensor node transmits its data by using the maximum available transmission power, which results in the highest possible k value of the network. The first case results in higher NLT when compared to the second case (up to 35% difference). However, the second case results in higher k-values (up to 20% difference) because increasing the transmission power increases the number of links, which in turn increases the k value of the network. Nevertheless, the model in [6] does not account for the maintenance cost of paths. Furthermore, the k value of the network is not a directly controllable parameter in the model presented in [6]. Indeed, the k value of a particular network topology is determined by a separate algorithm after nodes' transmission ranges are determined. For example, the optimization framework proposed in [6] can neither be utilized to determine NLT for a given k value (e.g., $k = 3$) nor it can model path maintenance costs.

The main contributions of this study are enumerated as follows:

1) To fill the gap in the literature we present an optimization framework, which is capable of maximizing UWSN lifetime for any given k value.
2) By employing the created optimization framework, we explore a large parameter space to quantitatively and systematically inspect the trade-off between k-connectivity and NLT in UWSNs, which has never been done in the literature, to the best of our knowledge.
3) Our results show that the extent of the tradeoff between k-connectivity maintenance and NLT has a strong dependence on the deployment scenario and system settings.

III. System Model

In this section, we introduce our network model (subsection III-A), present the energy dissipation model (subsection III-B), and elaborate on our optimization framework (subsection III-C). Table I presents the list of symbols and notations used in this paper.

A. Network Model

We consider a rectangular prism-shaped UWSN deployment topology with the width, length, and depth defined as d_x, d_y, and d_z, respectively (all in km). The network consists of $|W|$ battery-limited sensor nodes and a single BS (*i.e.*, node-1), where all data generated at the sensor nodes flow in. Hence the UWSN consists of $|V| = |W| + 1$ nodes in total. Note that W and V denote the sets of sensor nodes and all nodes, respectively, and $|.|$ is the cardinality of a set. Sensor nodes are randomly deployed within the network. On the other hand, the BS is floating on the water surface and positioned at one of the corners of the network. A sensor node can adjust its

TABLE I: The list of symbols and notations used in this paper.

Symbol	Description	Unit	Value	Symbol	Description	Unit	Value
A	Set of all links	–	–	a_{ij}^{kl}	Binary variable that shows whether the data generated by node-k on the path-l flows over the link-(i,j) or not	–	–
b_k^l	Total number of packets injected into the network by the source node-k on the path-l	packets	–	d_{ij}	Distance between node-i and node-j	m	–
d_x	Width of the network	km	1	d_y	Length of the network	km	$\{1, 2, 3\}$
d_z	Depth of the network	km	0.30	$E_T(\ell)$	Energy cost of transmission using the power level-ℓ	J/bit	–
$E_{T,ij}^*$	Optimum transmission energy for transmission over the link-(i,j)	J/bit	–	f	Center of operating frequency	kHz	25
G	Network graph	–	–	I_{jm}^i	Interference matrix	–	–
k_s	Spreading factor	–	1.5	$\mathcal{L}$	Set of discrete power levels	–	$\{1, \ldots, 10\}$
L_P	Packet size	bits	1024	M	Sufficiently large number	–	10^7
N_l	Total number of paths	–	5	N_R	Total number of rounds for network operation	–	3600
P_0	Desired power level at the input to the receiver	J/bit	1×10^{-7}	$E_R = P_r$	Reception constant	J/bit	0.2×10^{-7}
R_b	Data rate	bps	2500	$R_{\max}(\ell)$	Maximum transmission range at power level-ℓ	m	$\{100, \ldots, 1000\}$
s_k	Number of packets generated by node-k at each round	–	1	$TL(R_{\max}(\ell))$	Transmission loss over the distance $R_{\max}(\ell)$	–	–
T_R	Round duration	s	60	V	Set of all nodes including the BS	–	–
$\|V\|$	Total number of all nodes in the network	–	$\{20, 25, 30\}$	W	Set of all sensor nodes	–	–
$\|W\|$	Total number of sensor nodes in the network	–	$\{19, 24, 29\}$	x_{ij}^{kl}	Number of packets (of size L_P bits) generated by node-k, flowing over the link-(i,j) on path-l	–	–
$\alpha(f)$	Absorption coefficient	dB/km	–	γ	Interference range multiplier	–	1.7
κ	Reliability parameter (i.e., minimum required number of disjoint paths)	–	1–5	μ	Path maintenance parameter (i..e, the minimum fractions of data to be transmitted over each required path)	–	$\{0.05, 0.10, 0.20\}$
ν	Frequency-dependent component for calculating the transmission loss	–	–	ρ	Total energy dissipated by the most energy-hungry node	J	–
$\mathcal{D}_l$	Average weighted source-to-BS distance of path-l	km	–	$\mathcal{E}_l$	Average weighted energy dissipated per bit on path-l	mJ	–
$\mathcal{F}_l$	Average weighted number of packets traversing path-l	packets	–	$\mathcal{H}_l$	Average weighted source-to-BS hop count of path-l	–	–

transmission power level to be utilized for a particular link according to its distance to the destination node (denoted by d_{ij}, the distance between node-i and node-j, in m) using ten discrete power levels.

$\mathcal{L} = \{1, 2, \ldots, 10\}$ is defined as the set of all power levels. $R_{\max}(\ell)$ is the maximum transmission range (in m) when using the power level-ℓ ($\ell \in \mathcal{L}$).

The network is modeled as a graph, $G = (V, A)$, where $A = \{(i,j) : i \in W,\ j \in V \setminus \{i\},\ d_{ij} \leq R_{\max}(\ell = 10)\}$ is the ordered set of links. We assume that the time is organized into equal-duration time units (i.e. rounds) and the round duration is $T_R = 60$ s, which is a typical value in UWSNs [25]. In each round, each sensor node-k generates $s_k = 1$ packet of size $L_P = 1024$ bits. Data created by each sensor is conveyed to the BS either directly or by multi-hop routing. Each sensor node maintains, at least, κ (i.e., the reliability parameter) paths, which are disjoint (i.e., different paths of a sensor node do not share common links). Therefore, UWSNs explored in this study are k-connected in the sense that each sensor node has κ disjoint paths to the BS (i.e., $k = \kappa$).

As in the case of dynamic source routing (DSR) [26], each sensor node maintains its paths by periodically sending, at least, a certain fraction (μ, the path maintenance parameter) of its generated data over each link. For example, if $\mu = 0.1$, then each sensor node sends at least one data packet over each of its disjoint paths in every 10 rounds. The value of the maintenance parameter, μ, depends on the environment (i.e., a higher μ is needed in harsher environments to maintain the paths).

B. Underwater Energy Model

The underwater energy consumption model detailed in [27] is utilized throughout this work. When using the discrete power level-ℓ, a node can establish direct communication with other nodes, which are at most $R_{\max}(\ell)$ m away. In this case, the underwater path loss (attenuation) over the distance $R_{\max}(\ell)$ is expressed as

$$TL(R_{\max}(\ell)) = R_{\max}(\ell)^{k_s} \times \nu^{10^{-3} R_{\max}(\ell)}, \quad (1)$$

where $k_s = 1.5$, $\nu = 10^{\alpha(f)/10}$, $\alpha(f)$, and $f = 25$ kHz are the spreading factor for the practical cases, the frequency-dependent component, the absorption coefficient (in dB/km), and the center of operating frequency, respectively. $\alpha(f)$ is calculated using Thorp's formula as

$$\alpha(f) = \frac{0.11 f^2}{1 + f^2} + \frac{44 f^2}{4100 + f^2} + 2.75 \cdot 10^{-4} f^2 + 0.003. \quad (2)$$

Using the discrete power level-ℓ, transmitting a single bit costs

$$E_T(\ell) = TL(R_{\max}(\ell)) \times P_0, \quad (3)$$

of energy, where $P_0 = 1 \times 10^{-7}$ is the desired power level at the input to the receiver (J/bit) [27]. Furthermore, reception energy cost of a single bit is constant, which is defined as

$$E_R = P_r, \quad (4)$$

where $P_r = 0.2 \times 10^{-7}$ is the reception constant (J/bit) [27]. In Table II, we present the transmission energy costs (*i.e.*, $E_T(\ell)$ in mJ/bit) and the transmission ranges (*i.e.*, $R_{\max}(\ell)$ in meters) for each power level-ℓ.

TABLE II: The transmission energy cost ($E_T(\ell)$ – mJ/bit) and the communication range ($R_{\max}(\ell)$ – m) at power level-ℓ when $f = 25$ kHz and $k_s = 1.5$.

ℓ	$E_T(\ell)$	$R_{\max}(\ell)$	ℓ	$E_T(\ell)$	$R_{\max}(\ell)$
1	0.115	100	6	3.416	600
2	0.375	200	7	4.954	700
3	0.792	300	8	6.967	800
4	1.404	400	9	9.568	900
5	2.258	500	10	12.897	1000

Each node-i can control its transmission power according to the distance between the transmitter (*i.e.*, node-i) and the receiver (*i.e.*, node-j). The optimum transmission energy cost over the link-(i,j) is calculated as

$$E^*_{T,ij} = \begin{cases} E_T(\ell=1), \text{ if } d_{ij} \le R_{\max}(\ell=1) \\ \infty, \text{ if } d_{ij} \ge R_{\max}(\ell=10) \\ E_T(\ell+1), \text{ if } R_{\max}(\ell) \le d_{ij} \le R_{\max}(\ell+1) \end{cases}. \tag{5}$$

For instance, assume that the distance between node-2 and node-5 is 520 meters. Since 500 m $<$ d_{25} $=$ 520 m $\le$ 600 m, node-2 should use power level-6 for communicating with node-5, where the optimum energy cost for transmitting a single bit is $E^*_{T,25} = E_T(\ell=6) = 3.416$ mJ.

C. MILP Model for the Minimum Energy Consumption

The mixed-integer linear programming (MILP) model aims to determine the optimal multi-path routes and the number of data packets transferred on each path for minimizing the energy dissipation. More specifically, energy dissipation of the maximum energy dissipating node (i.e., The highest energy dissipating node - THEDN) is minimized. The objective function, which minimizes the total energy dissipated by THEDN (*i.e.*, ρ), is presented in (6a). In our model, each sensor node generates a single data packet at each round for a total 3600 rounds (i.e., $N_R = 3600$ rounds), which is 60 hours.

Note that minimizing the energy consumption of THEDN is equivalent to maximizing NLT [28], [29]. Therefore, it is straightforward to determine NLT for a UWSN with sensor nodes having the same battery energy at the beginning of the network operation by using the solution of our optimization model (i.e., NLT equals to 3600 times the ratio of the battery energy to the energy dissipated by THEDN). Nevertheless, ρ and NLT are inversely proportional, therefore, to maximize the lifetime ρ should be minimized, which is the objective of our optimization framework.

The constraints of the MILP model are given in (6b)–(6r). The decision variables of the MILP framework are as follows:

- x^{kl}_{ij}: Integer variable that models the number of packets (of size L_P bits) generated by node-k, flowing over the link-(i,j) on path-l.
- b^l_k: Integer variable defined as the total number of packets injected into the network by the source node-k on path-l.
- a^{kl}_{ij}: Binary variable that shows whether the data generated by node-k on path-l flows over the link-(i,j) or not.

Minimize ρ (6a)

subject to:

$$\sum_{(i,j)\in A} x^{kl}_{ij} - \sum_{(j,i)\in A} x^{kl}_{ji} = \begin{cases} b^l_k & \text{if } i = k \\ -b^l_k & \text{if } i = 1 \\ 0 & \text{o.w.} \end{cases}, \quad \forall i \in V,\ k \in W,\ l = \{1,\dots,N_l\} \tag{6b}$$

$$\sum_{l=1}^{N_l} b^l_k = s_k \times N_R, \quad \forall k \in W \tag{6c}$$

$$\sum_{j\in W} x^{kl}_{jk} = 0, \quad \forall k \in W,\ l = \{1,\dots,N_l\} \tag{6d}$$

$$x^{kl}_{ij} \le s_k \times N_R \times a^{kl}_{ij}, \quad \forall (i,j) \in A,\ k \in W, \ l = \{1,\dots,N_l\} \tag{6e}$$

$$a^{kl}_{ij} \le x^{kl}_{ij}, \quad \forall (i,j) \in A,\ k \in W,\ l = \{1,\dots,N_l\} \tag{6f}$$

$$\sum_{(i,j)\in A} a^{kl}_{ij} \le 1, \quad \forall i \in W,\ k \in W,\ l = \{1,\dots,N_l\} \tag{6g}$$

$$\sum_{l=1}^{N_l} a^{kl}_{ij} \le 1, \quad \forall (i,j) \in A,\ k \in W \tag{6h}$$

$$\sum_{(j,1)\in A} x^{k(l+1)}_{j1} \le \sum_{(j,1)\in A} x^{kl}_{j1}, \quad \forall k \in W,\ l = \{1,\dots,N_l - 1\} \tag{6i}$$

$$\sum_{(k,j)\in A} \sum_{l=1}^{N_l} a^{kl}_{kj} \ge \kappa, \quad \forall k \in W \tag{6j}$$

$$x^{kl}_{ij} \ge \mu \times s_k \times N_R \times a^{kl}_{ij}, \quad \forall (i,j) \in A,\ k \in W, \ l = \{1,\dots,N_l\} \tag{6k}$$

$$x^{kl}_{ij} - M(1 - a^{kl}_{ij}) \le b^l_k, \quad \forall (i,j) \in A,\ k \in W, \ l = \{1,\dots,N_l\} \tag{6l}$$

$$x^{kl}_{ij} + M(1 - a^{kl}_{ij}) \ge b^l_k, \quad \forall (i,j) \in A,\ k \in W, \ l = \{1,\dots,N_l\} \tag{6m}$$

$$L_P \sum_{l=1}^{N_l} \sum_{k\in W} \left(\sum_{(i,j)\in A} E^*_{T,ij} x^{kl}_{ij} + \sum_{(j,i)\in A} E_R x^{kl}_{ji} \right) \le \rho, \quad \forall i \in W \tag{6n}$$

$$\frac{L_P}{R_b} \sum_{k\in W} \sum_{l=1}^{N_l} \left(\sum_{(i,j)\in A} x^{kl}_{ij} + \sum_{(j,i)\in A} x^{kl}_{ji} + \sum_{(j,m)\in A\setminus\{i\}} x^{kl}_{jm} I^i_{jm} \right) \le N_R \times T_R, \quad \forall i \in V \tag{6o}$$

$$x^{kl}_{ij} \ge 0, \quad \forall (i,j) \in A,\ k \in W,\ l = \{1,\dots,N_l\} \tag{6p}$$

$$a^{kl}_{ij} \in \{0,1\}, \quad \forall (i,j) \in A,\ k \in W,\ l = \{1,\dots,N_l\} \tag{6q}$$

$$b^l_k \ge 0, \quad \forall k \in W,\ l = \{1,\dots,N_l\} \tag{6r}$$

Constraint (6b) conserves flows at each source node ($i = k$), the BS ($i = 1$), and each relay node ($i \neq k$). Constraint (6c)

assures that each source node-k generates a total of $s_k \times N_R$ packets. Note that the total number of packets generated by source node-k can be routed to the BS using at most N_l paths (multi-path routing). The set $l = \{1, \ldots, N_l\}$ is an index set, which is utilized to identify disjoint paths for each sensor node. Links constituting a path are determined by the optimization model. Therefore, the set of paths are not predefined but determined by solving the optimization model.

Constraint (6d) guarantees that the data generated at source node-k and routed out to the rest of the network does not loop back to the source node-k. Constraint (6e) and constraint (6f) jointly determine the value of the indicator binary variable a_{ij}^{kl}, which is one if the link-(i, j) is used for carrying the data generated by the source node-k on its l-th path, otherwise, it is zero (*i.e.*, $a_{ij}^{kl} = 1$ if $x_{ij}^{kl} > 0$ and $a_{ij}^{kl} = 0$ if $x_{ij}^{kl} = 0$). Constraint (6g) guarantees that the flow on each path is non-bifurcated such that there should be only a single next-hop node, which can either be the BS or another relay node. This constraint constructs a non-branching path from source nodes to the BS for conveying the data. Constraint (6h) imposes that data packets, originated at source node-k, flowing over each link-(i, j), can belong to at most one of node-k's N_l paths. Note that constraint (6g) enforces that each source-to-BS path is not forked at any node constituting the path, whereas constraint (6h) guarantees that all paths originating at each source node are disjoint.

Constraint (6i) enforces that the number of packets generated by the source node-k transported on path-l is greater than or equal to the number of packets transmitted on its $(l + 1)^{\text{th}}$ path (i.e., the number of packets is a non-increasing function of l). Note that this constraint is not necessary for the optimization purpose, however, it is helpful in the analysis (Section IV).

Constraint (6j) imposes the k-connectivity criterion, which states that the data generated by the sensor node-k must have at least κ different paths for reaching the BS. In fact, constraint (6j) along with constraint (6h) guarantees that each sensor node maintains, at least, κ disjoint paths to the BS. Constraint (6k) provides the lower bound on the flows, which must be at least $\mu \times s_k \times N_R$ (i.e., μ times the total number of packets generated at each sensor node). Indeed, μ is the parameter that quantifies the maintenance cost of the extra paths in our framework. We investigate the impact of varying the parameter, μ between 0.05 to 0.20 on ρ in Section IV. Constraint (6l) and constraint (6m) are included in the optimization framework to eliminate the possible phantom flows (i.e., subtours) [30], which are invalid flows that do not violate constraint (6b), the flow conservation constraint, (i.e., flows that do not terminate at the BS) and M is a sufficiently large number. Constraint (6n) is used to assign the THEDN's energy (energy consumed for transmission and reception by node-i) to the objective function to be minimized (i.e., ρ). Note that THEDN is not known before the optimization problem for a specific instance is solved. In fact, THEDN and ρ are determined once the problem is solved to optimality. Constraint (6o) is the bandwidth constraint such that the bandwidth used for transmission, reception, and silent waiting (due to transmissions of nearby nodes) is limited to the available channel bandwidth (R_b). In this constraint, I_{jm}^i is a binary parameter, which takes the value, 1, if node-i is in the interference region of the communication between node-j and node-m (*i.e.*, node-i cannot receive from any other node while node-j transmits to node-m provided that $\gamma d_{jm} \geq d_{ji}$), and 0, otherwise. I_{jm}^i is calculated as follows

$$I_{jm}^i = \begin{cases} 1 & \text{if } \gamma d_{jm} \geq d_{ji} \ \forall j \in W, \ \forall m \in V \setminus \{j\} \\ 0 & \text{otherwise} \end{cases}, \quad (7)$$

where $\gamma = 1.7$ is the interference range multiplier [31]. Constraints (6p)–(6r) define the bounds of the decision variables.

IV. Analysis

In this section, we present the results of our analysis, which are based on the numerical evaluations of the optimization model presented in subsection III-C, spanning a comprehensive parameter space. Our main purpose is to characterize the trade-off between ρ, which is inversely proportional to NLT as explained in subsection III-C in detail, and network reliability in terms of k-connectivity (i.e., κ). All the parameters utilized in our analysis are presented in Table I and Table II.

We performed our investigation under three carefully designed scenarios, which are employed to characterize the trade-off between energy dissipation and reliability as two of the parameters change while the other parameters are kept constant:

- **Scenario-I:** In this scenario, the number of nodes and the path maintenance parameter are fixed (i.e., $|V| = 20$ and $\mu = 0.10$) while the length of the deployment area, d_y, is varied from 1 km to 3 km. As such, the results of this scenario enables us to observe the effects of increasing both number of hops from the source nodes to the BS (the average and the maximum) and the reliability parameter, κ, on ρ.
- **Scenario-II:** The second scenario is designed to be able to observe the impact of node density and κ on ρ, where the dimensions of the deployment topology and μ are kept constant (i.e., $d_y = 2$ km and $\mu = 0.10$) while the number of nodes ($|V|$) varied from 20 to 30.
- **Scenario-III:** The third scenario focuses on the impact of the variation of the path maintenance parameter, μ, which takes values from 0.05 to 0.20 (e.g., if $\mu = 0.05$ then all sensor nodes are required to send, at least, 5% of their generated data from each of their paths) and κ on ρ. The other parameters are frozen in this scenario (i.e., $|V| = 20$ nodes and $d_y = 2$ km).

Note that in all scenarios dimensions of the deployment topology other than the length (i.e., d_y) are fixed (i.e., $d_x = 1$ km and $d_z = 0.3$ km). Furthermore, in all scenarios the reliability parameter, κ, is varied from 1 to 5.

The network and the underwater energy consumption models are constructed in MATLAB, while the MILP model formulated in Section (III-C) is solved to optimality using General Algebraic Modeling System (GAMS) with CPLEX solver [32]. Throughout this section, the data points presented in Figs. 1–5 are the averages of the results obtained with 50 randomly generated deployment instances.

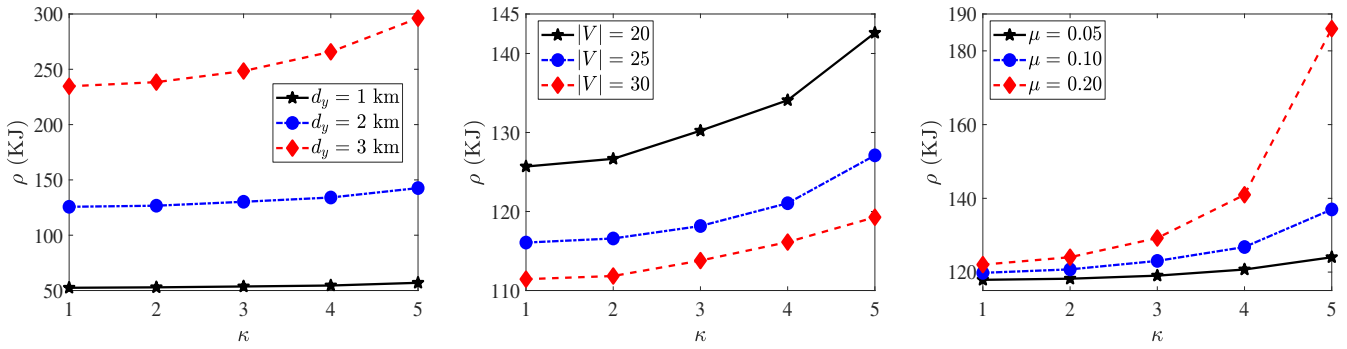

(a) Scenario-I (b) Scenario-II (c) Scenario-III

Fig. 1: Energy dissipation (ρ) vs. κ by varying: (a) UWSN deployment length (d_y), (b) number of nodes ($|V|$), and (c) maintenance parameter (μ).

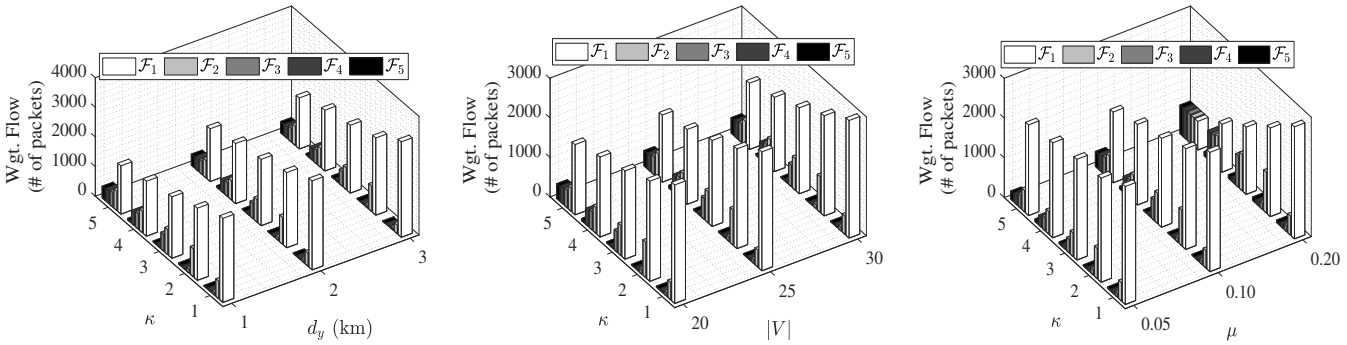

(a) Scenario-I (b) Scenario-II (c) Scenario-III

Fig. 2: Average weighted traffic flow (number of packets) per path vs.: (a) κ & d_y, (b) κ & $|V|$, and (c) κ & μ.

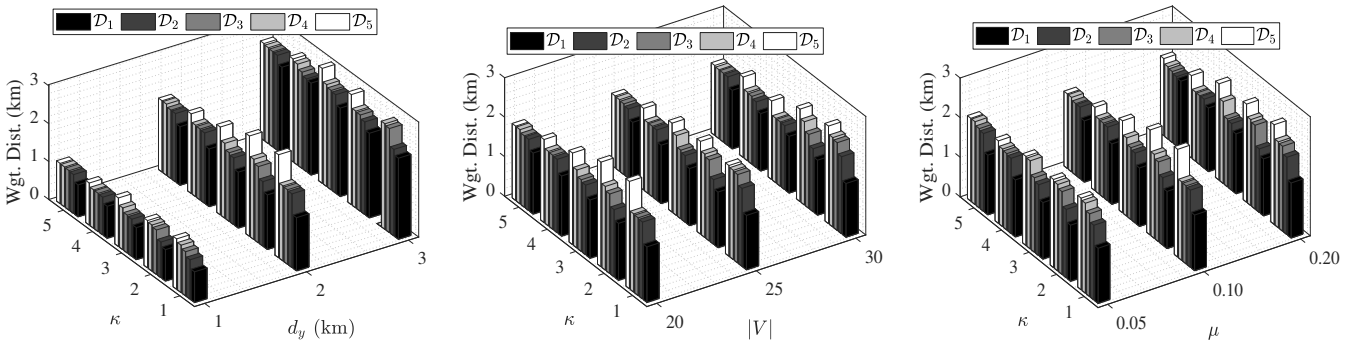

(a) Scenario-I (b) Scenario-II (c) Scenario-III

Fig. 3: Average weighted source-to-BS distances of paths vs.: (a) κ & d_y, (b) κ & $|V|$, and (c) κ & μ.

Energy dissipation values of THEDN, ρ, as functions of κ are presented in Fig. 1. More specifically, Figs. 1a, 1b, and 1c, present the trade-off between ρ and κ for different values of UWSN deployment length, d_y (Scenario-I), number of nodes, $|V|$ (Scenario-II), and maintenance parameter, μ (Scenario-III), respectively. The first observation from Figs. 1a, 1b, and 1c is that the energy dissipation, ρ, increases as κ gets larger. For example, in Fig. 1a, when $d_y = 3$ km, ρ values are 234.64, 238.39, 248.44, 265.80, and 296.24 (all in kJ) for $\kappa = 1$, 2, 3, 4, and 5, respectively. The reason for such behavior is that unless forced to disperse their generated data into a higher number of disjoint paths, sensor nodes tend to convey most of their data packets with their first paths as illustrated in Fig. 2. In fact, longer distances (both the actual path distance in km and the hop distance) are traversed by the packets in extra paths, which is aggravated by the k-connectivity constraint, as revealed by the data presented in Figs. 3 and 4. Furthermore, the energy cost of conveying packets in the extra paths also gets larger in accordance with the path number, l, as revealed in Fig. 5.

For Scenario-I (Fig. 1a), ρ increases as the network size grows (*i.e.*, when d_y increases) since the energy needed for transmission increases as the source-to-destination distance increases. For instance, when $\kappa = 2$, ρ values are 52.87, 126.67, and 238.39 kJ for $d_y = 1$, 2, and 3 km, respectively. For Scenario-II (Fig. 1b), ρ increases as the number of nodes,

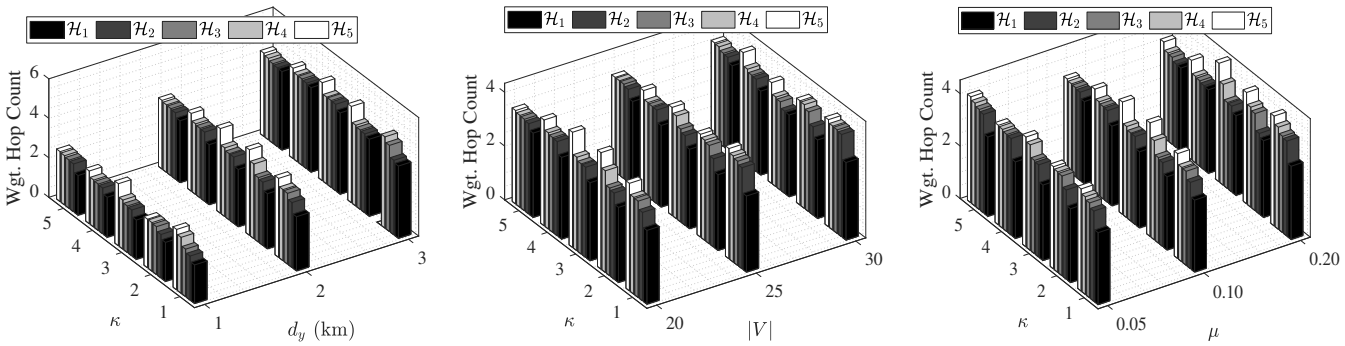

(a) Scenario-I (b) Scenario-II (c) Scenario-III

Fig. 4: Average weighted end-to-end hop counts of paths vs.: (a) κ & d_y, (b) κ & $|V|$, and (c) κ & μ.

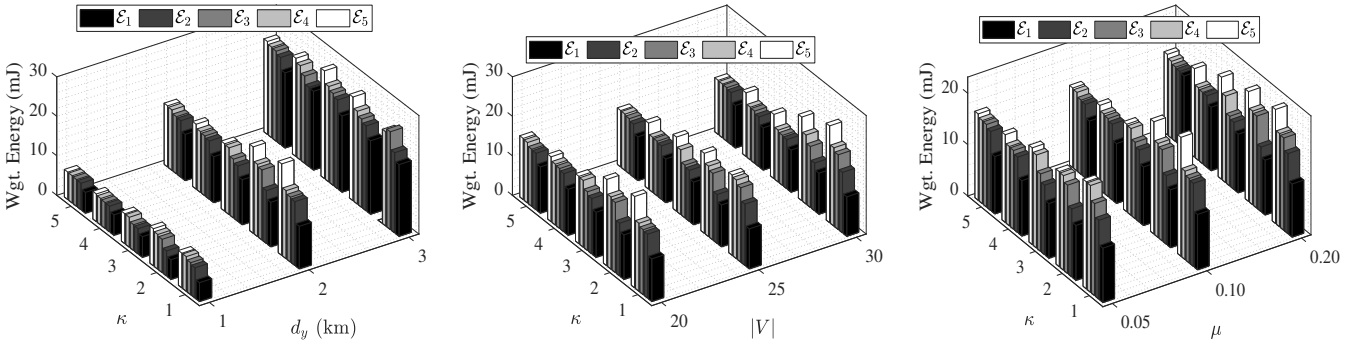

(a) Scenario-I (b) Scenario-II (c) Scenario-III

Fig. 5: Average weighted energy dissipation per path per bit vs.: (a) κ & d_y, (b) κ & $|V|$, and (c) κ & μ.

$|V|$, decreases (network dimensions are kept constant) because as $|V|$ decreases the average inter-node distance increases, which leads to higher per hop energy dissipation. For example, when $\kappa = 5$, ρ values increase from 119.28 kJ to 142.61 kJ as $|V|$ decreases from 30 to 20. For Scenario-III (Fig. 1c), ρ increases as μ increases since nodes need to guarantee to transmit higher percentage of their generated data on less energy efficient paths, culminating in extra energy burden on the nodes. Nevertheless, as the k-connectivity criterion gets more demanding as κ increases from 1 to 5, ρ increases in the intervals of 8.58%–26.25%, 7.03%–13.46%, and 5.19%–52.45%, for Scenario-I, Scenario-II, and Scenario-III, respectively.

Since NLT is one of the most important performance metrics for UWSNs, establishing the relationship between NLT and ρ is necessary. As such, we would like to emphasize the fact that the increase in ρ in a UWSN is directly related (i.e., inversely proportional) to the amount of reduction in NLT. For example, if ρ increases by 50% then NLT decreases by approximately 33% (i.e., $1 - \frac{1}{1.5} = 0.33$) [33].

In Fig. 2, average weighted traffic (*i.e.*, the number of packets) per path values are presented for Scenario-I (Fig. 2a), Scenario-II (Fig. 2b), and Scenario-III (Fig. 2c) as functions of κ, d_y, $|V|$, and μ. The average weighted flow over each path-l (*i.e.*, $\mathcal{F}_l$) is defined as

$$\mathcal{F}_l = \frac{\sum_{k \in W} b_k^l}{\sum_{k \in W} \sum_{(k,j) \in A} a_{kj}^{kl}}, \; l = \{1, \ldots, N_l\}. \qquad (8)$$

Note that summation over $(k, j) \in A$ restricts the summation over the outgoing links of source node-k, only. For calculating $\mathcal{F}_l$, we use the optimal solutions of the decision variables a_{ij}^{kl}, x_{kj}^{kl}, and b_k^l that yield the minimum ρ. We provide five group bars for each parameter set, where each bar shows the average weighted traffic of path-l. Regardless of the scenario or the parameter configuration, $\sum_{l=1}^{N_l=5} \mathcal{F}_l = 3600$, since each sensor node-k generates a total of 3600 packets to be delivered to the BS (*i.e.*, $s_k \times N_R = 3600$). The upper limit on the number of paths, N_l, is 5 because F_l is negligible for $l > 5$. Even for low values of κ (e.g., $\kappa = 1$), there are non-zero flows in the paths other than the first path because nodes use the alternate paths to balance the energy dissipation throughout the network so that ρ is minimized, which determines NLT. However, unless the nodes are forced to spread their data on alternative paths, most of the traffic flows by using the first path, which is the shortest and least energy consuming path as revealed by Figs. 3, 4, and 5. For example, in Scenario-II (Fig. 2b) with $\kappa = 1$ and $|V| = 25$, $\mathcal{F}_1 = 3014.80$ (83.74% of the total flow), $\mathcal{F}_2 = 429.43$, $\mathcal{F}_3 = 89.61$, $\mathcal{F}_4 = 42.60$, and $\mathcal{F}_5 = 23.53$ (less than 0.01% of the total flow). However, when $\kappa = 5$ and $\mu = 0.20$ (Fig. 2c), $\mathcal{F}_1 = \ldots = \mathcal{F}_5 = 720$ packets because all sensor nodes are forced to send 20.00% of their packets on each of the five paths, which is the parameter set where ρ is the highest for this scenario (*i.e.*, $\rho = 186.02$ kJ).

In Fig. 3, the average weighted distance of each path (*i.e.*, the average weighted distance between source nodes and the

BS) is provided (in km) for Scenario-I (Fig. 3a), Scenario-II (Fig. 3b), and Scenario-III (Fig. 3c). The average weighted distance of path-l (*i.e.*, $\mathcal{D}_l$) is calculated as

$$\mathcal{D}_l = \frac{\sum_{k\in W}\sum_{(i,j)\in A} x_{ij}^{kl} d_{ij}}{\sum_{k\in W}\sum_{(k,j)\in A} x_{kj}^{kl}},\ l = \{1,\ldots,N_l\}. \quad (9)$$

As a general trend, *i.e.*, $\mathcal{D}_1 \leq \mathcal{D}_2 \leq \ldots \leq \mathcal{D}_5$ in all scenarios. For example, when $\kappa = 5$ and $d_y = 3$ km (Fig. 3a), $\mathcal{D}_l$ values are obtained as 2.28, 2.51, 2.52, 2.54, 2.56 (all in km) for $l = 1$, 2, 3, 4, and 5, respectively. Since $\mathcal{F}_l \geq \mathcal{F}_{l+1}$, to minimize the energy dissipation, nodes choose shorter paths for conveying more traffic.

In Fig. 4, the average weighted source-to-BS hop count values (*i.e.*, $\mathcal{H}_l$) are shown for each path-l for all three scenarios (Figs. 4a, 4b, and 4c). $\mathcal{H}_l$ is calculated as follows

$$\mathcal{H}_l = \frac{\sum_{k\in W}\sum_{(i,j)\in A} x_{ij}^{kl}}{\sum_{k\in W}\sum_{(k,j)\in A} x_{kj}^{kl}},\ l = \{1,\ldots,N_l\}. \quad (10)$$

As in the case of source-to-BS distance, source-to-BS hop count also increases with increasing κ (i.e., $\mathcal{H}_1 \leq \mathcal{H}_2 \leq \ldots \leq \mathcal{H}_5$), as a general trend, which also indicates that higher κ values lead to higher average end-to-end delay. For example, in Scenario-III (Fig. 4c) with $\kappa = 5$ and $\mu = 0.2$, $\mathcal{H}_1 = 3.17$, $\mathcal{H}_2 = 3.19$, $\mathcal{H}_3 = 3.32$, $\mathcal{H}_4 = 3.36$, and $\mathcal{H}_5 = 3.65$.

Fig. 5 presents the average weighted source-to-BS energy dissipation per path per bit, $\mathcal{E}_l$, for all scenarios, which is obtained as

$$\mathcal{E}_l = \frac{\sum_{k\in W}\sum_{(i,j)\in A} x_{ij}^{kl}\left(E_{T,ij}^{*} + E_R\right)}{\sum_{k\in W}\sum_{(k,j)\in A} x_{kj}^{kl}},\ l = \{1,\ldots,N_l\}. \quad (11)$$

In all scenarios $\mathcal{E}_l$ increases as l increases because the path length also increases with l as well (i.e., to minimize energy dissipation it is the best decision to utilize shorter paths, in general).

V. Conclusion

In this study, we present a systematic analysis of the trade-off between k-connectivity based network reliability and lifetime maximization. We create a novel MILP framework to model both the energy dissipation of the highest energy dissipating node and the k value to be maintained in a UWSN. Through the solutions of the MILP model spanning a large parameter space, we achieve a thorough characterization of the aforementioned trade-off. The results of this study reveal that the impact of the k value on network lifetime depends, strongly, on UWSN deployment and operation parameters. In a UWSN with the parameter set of $\mu = 0.2$, $|V| = 20$, $d_x = 1$ km, $d_x = 2$ km, and $d_z = 0.3$ km, maintaining a 5-connected UWSN increases the energy dissipation more than 50.00%, which means more than 33.00% decrease in network lifetime, when compared to a 1-connected UWSN with the same parameter set. On the other hand, in another UWSN with the parameter set of $\mu = 0.1$, $|V| = 30$, $d_x = 1$ km, $d_x = 2$ km, and $d_z = 0.3$ km, it is also possible to maintain a 3-connected network with less than 2.11% increase in energy dissipation (less than 2.07% decrease in lifetime) when compared to a 1-connected network with the same parameter set. Nevertheless, our main conclusion is that maintaining k-connectivity can result in significant reduction in network lifetime. The results we present can be used as guidelines in designing UWSNs according to both lifetime and reliability requirements. Verification of the results we obtained in this study through direct testbed experimentation is an interesting open research topic.

References

[1] T. Qiu, Z. Zhao, T. Zhang, C. Chen, and C. L. P. Chen, "Underwater internet of things in smart ocean: System architecture and open issues," *IEEE Trans. Ind. Informat.*, vol. 16, no. 7, pp. 4297–4307, Jul. 2020.

[2] J. Luo, Y. Chen, M. Wu, and Y. Yang, "A survey of routing protocols for underwater wireless sensor networks," *IEEE Commun. Surveys Tuts.*, vol. 23, no. 1, pp. 137–160, Firstquarter 2021.

[3] X. Wei, H. Guo, X. Wang, X. Wang, and M. Qiu, "Reliable data collection techniques in underwater wireless sensor networks: A survey," *IEEE Commun. Surveys Tuts.*, pp. 1–29, 2022.

[4] H. U. Yildiz, V. C. Gungor, and B. Tavli, "Packet size optimization for lifetime maximization in underwater acoustic sensor networks," *IEEE Trans. Ind. Informat.*, vol. 15, no. 2, pp. 719–729, Feb. 2019.

[5] A. Vavoulas, H. G. Sandalidis, and D. Varoutas, "Underwater optical wireless networks: A k-connectivity analysis," *IEEE J. Ocean. Eng.*, vol. 39, no. 4, pp. 801–809, Oct. 2014.

[6] M. Cobanlar, V. K. Akram, O. Dagdeviren, and B. Tavli, "Analysis of the tradeoff between network lifetime and k-connectivity in WSNs," in *Proc. Telecommun. Forum (TELFOR)*, 2018, pp. 1–4.

[7] W. Mo, D. Qiao, and Z. Wang, "Lifetime maximization of sensor networks under connectivity and k-coverage constraints," in *Lecture Notes in Computer Science (Proc. Distributed Computing in Sensor Systems – DCOSS)*, P. Gibbons, T. Abdelzaher, J. Aspnes, and R. Rao, Eds. Berlin, Heidelberg: Springer, 2006, vol. 4026, pp. 422–442.

[8] H. Sheikhi, M. Hoseini, and M. Sabaei, "k-connected relay node deployment in heterogeneous wireless sensor networks," *Wireless Pers. Commun.*, vol. 120, pp. 1–16, Oct. 2021.

[9] Z. Yun, X. Bai, D. Xuan, T. H. Lai, and W. Jia, "Optimal deployment patterns for full coverage and k-connectivity ($k \leq 6$) wireless sensor networks," *IEEE/ACM Trans. Netw.*, vol. 18, no. 3, pp. 934–947, Jun. 2010.

[10] A. Zrelli and T. Ezzedine, "A new approach of WSN deployment, k-coverage and connectivity in border area," *Wireless Pers. Commun.*, vol. 121, pp. 3365—-3381, Dec. 2021.

[11] A. Tripathi, H. P. Gupta, T. Dutta, R. Mishra, K. Shukla, and S. Jit, "Coverage and connectivity in WSNs: A survey, research issues and challenges," *IEEE Access*, vol. 6, pp. 26 971–26 992, Jun. 2018.

[12] M. Navarro, T. W. Davis, Y. Liang, and X. Liang, "A study of long-term WSN deployment for environmental monitoring," in *Proc. IEEE Ann. Int. Symp. Pers. Indoor Mobile Radio Commun. (PIMRC)*, 2013, pp. 2093–2097.

[13] R. Singh and M. S. Manu, "An energy efficient grid based static node deployment strategy for wireless sensor networks," *Int. J. Electron. Informat. Eng.*, vol. 7, no. 1, pp. 32–40, Sept. 2017.

[14] B. S. Panda and D. P. Shetty, "Minimum range assignment problem for two connectivity in wireless sensor networks," in *Proc. Int. Conf. Distrib. Comput. Internet Techn. (ICDCIT)*, 2014, pp. 122–133.

[15] H. Bagci, I. Korpeoglu, and A. Yazici, "A distributed fault-tolerant topology control algorithm for heterogeneous wireless sensor networks," *IEEE Trans. Parallel Distrib. Syst.*, vol. 26, no. 4, pp. 914–923, Apr. 2014.

[16] V. K. Akram, O. Dagdeviren, and B. Tavli, "A coverage-aware distributed k-connectivity maintenance algorithm for arbitrarily large k in mobile sensor networks," *IEEE/ACM Trans. Netw.*, vol. 30, no. 1, pp. 62–75, Feb. 2022.

[17] V. K. Akram and O. Dagdeviren, "DECK: A distributed, asynchronous and exact k-connectivity detection algorithm for wireless sensor networks," *Comput. Commun.*, vol. 116, pp. 9–20, Jan. 2018.

[18] O. Dagdeviren and V. K. Akram, "PACK: Path coloring based k-connectivity detection algorithm for wireless sensor networks," *Ad Hoc Netw.*, vol. 64, pp. 41–52, Jun. 2017.

[19] M. R. Henzinger, S. Rao, and H. N. Gabow, "Computing vertex connectivity: New bounds from old techniques," *J. Algorithms*, vol. 34, no. 2, pp. 222–250, Feb. 2000.

[20] A. Cornejo and N. Lynch, "Fault-tolerance through k-connectivity," in *Proc. Workshop Netw. Sci. Sys. Issues Multirobot Autonomy (ICRA)*, vol. 2, 2010, pp. 1–4.

[21] M. Jorgic, N. Goel, K. Kalaichevan, A. Nayak, and I. Stojmenovic, "Localized detection of k-connectivity in wireless ad hoc, actuator and sensor networks," in *Proc. Int. Conf. Comput. Commun. Netw. (ICCCN)*, 2007, pp. 33–38.

[22] O. Dagdeviren, V. K. Akram, and B. Tavli, "Design and evaluation of algorithms for energy efficient and complete determination of critical nodes for wireless sensor network reliability," *IEEE Trans. Rel.*, vol. 68, no. 1, pp. 280–290, Mar. 2019.

[23] S. Lee, M. Younis, and M. Lee, "Connectivity restoration in a partitioned wireless sensor network with assured fault tolerance," *Ad Hoc Netw.*, vol. 24, pp. 1–19, Jan. 2015.

[24] V. K. Akram, O. Dagdeviren, and B. Tavli, "Distributed k-connectivity restoration for fault tolerant wireless sensor and actuator networks: algorithm design and experimental evaluations," *IEEE Trans. Rel.*, vol. 70, no. 3, pp. 1112–1125, Sept. 2021.

[25] S. Climent, J. V. Capella, S. Blanc, A. Perles, and J. J. Serrano, "A proposal for modeling real hardware, weather and marine conditions for underwater sensor networks," *MDPI Sensors*, vol. 13, no. 6, pp. 7454–7471, Jun. 2013.

[26] S. Kurumbanshi, S. Rathkanthiwar, S. Patil, and P. Wararkar, "Deployment of energy efficient network using dynamic source routing," in *Proc. Int. Conf. Comput. Commun. Informat. (ICCCI)*, 2021, pp. 1–5.

[27] M. A. Khan, N. Javaid, A. Majid, M. Imran, and M. Alnuem, "Dual sink efficient balanced energy technique for underwater acoustic sensor networks," in *Proc. Int. Conf. Adv. Inform. Netw. Appl. Work. (WAINA)*, 2016, pp. 551–556.

[28] R. Madan and S. Lall, "Distributed algorithms for maximum lifetime routing in wireless sensor networks," *IEEE Trans. Wirel. Commun.*, vol. 5, no. 8, pp. 2185–2193, Aug. 2006.

[29] J. Zhu, K.-L. Hung, and B. Bensaou, "Tradeoff between network lifetime and fair rate allocation in wireless sensor networks with multi-path routing," in *Proc. ACM Int. Symp. Model. Anal. Simul. Wirel. Mobile Syst. (MSWiM)*, 2006, pp. 301–308.

[30] T. Bektas and L. Gouvei, "Requiem for the Miller–Tucker–Zemlin subtour elimination constraints?" *Eur. J. Oper. Res.*, vol. 236, no. 3, pp. 820–832, Aug. 2014.

[31] M. Cheng, X. Gong, and L. Cai, "Joint routing and link rate allocation under bandwidth and energy constraints in sensor networks," *IEEE Trans. Wirel. Commun.*, vol. 8, no. 7, pp. 3770–3779, Jul. 2009.

[32] "General Algebraic Modeling System (GAMS)," http://www.gams.com/, accessed: 2022-04-29.

[33] H. Cotuk, B. Tavli, K. Bicakci, and M. B. Akgun, "The impact of bandwidth constraints on the energy consumption of wireless sensor networks," in *Proc. IEEE Wireless Commun. Network. Conf. (WCNC)*, 2014, p. 2787–2792.

Muhammed Cobanlar received the B.Sc. and M.Sc. degrees from Izmir Institute of Technology, Izmir, Turkey, in 2010 and 2014, respectively, both in Electronics and Communication Engineering. He is currently pursuing his Ph.D. in Electrical and Electronics Engineering at TOBB University of Economics and Technology, Ankara, Turkey. His research interest include, computer networks, wireless communications, and optimization.

Huseyin Ugur Yildiz received the B.Sc. degree from Bilkent University, Ankara, Turkey, in 2009; the M.Sc. and Ph.D. degrees from TOBB University of Economics and Technology, Ankara, in 2013 and 2016, respectively, all in electrical and electronics engineering. He is an associate professor in the department of electrical and electronics engineering at TED University, Ankara. His research focuses on the applications of optimization techniques for modeling and analyzing research problems on underwater wireless sensor networks.

Vahid Khalilpour Akram received the B.Sc. and the M.Sc. degrees in Computer Engineering from Islamic Azad University, Tehran, Iran. He received Ph.D. degree from Ege University, International Computer Institute, Izmir, Turkey. He currently is an assistant professor at Ege University, International Computer Institute, Izmir. His research interests include wireless sensor networks, parallel and distributed algorithms, and graph theory.

Orhan Dagdeviren received the B.Sc. and the M.Sc. degrees in Computer Engineering from Izmir Institute of Technology, Izmir, Turkey. He received Ph.D. degree from Ege University, International Computer Institute, Izmir. He is an associate professor and is the director of Network Science Laboratory in International Computer Institute, Izmir. His interests lie in the distributed computing, applied graph theory, and computer networking areas.

Bulent Tavli received his Ph.D. degree in electrical engineering from the University of Rochester, Rochester, NY, USA, in 2005. He is currently a professor with the department of electrical and electronics engineering, TOBB University of Economics and Technology, Ankara, Turkey. His research interests include network science, algorithm design and analysis, telecommunications, privacy and security, smart grids, embedded systems, optimization, machine learning, digital twins, and blockchain.